IEEE Access
Multidisciplinary | Rapid Review | Open Access Journal

Received September 16, 2018, accepted October 7, 2018, date of publication October 12, 2018, date of current version November 9, 2018.

Digital Object Identifier 10.1109/ACCESS.2018.2875786

A Multi-Objective Robust Optimization Design for Grid Emergency Goods Distribution Under Mixed Uncertainty

YIWEN JIANG, LEE LI, (Senior Member, IEEE), AND ZHENSHENG LIU
School of Electrical and Electronic Engineering, Huazhong University of Science and Technology, Wuhan 430074, China

Corresponding author: Lee Li (leeli@hust.edu.cn)

This work was supported by the National Natural Science Fund of China under Grant 51777082.

ABSTRACT Emergency goods distribution plays an important role in the grid emergency relief command system. However, the traditional experience-based distribution plan currently in the power grid cannot meet the increasing demand for the types and quantities of emergency goods, meanwhile, most studies ignore the uncertainty in distribution parameters and diversification of distribution objectives, which causes a gap between theoretical research and practical application. Therefore, this paper establishes a model to guide the logistics design for transferring relief supplies. The model first assesses the importance of affected areas for determining distribution priority based on the electrical characteristics. To better simulate reality, the uncertainties in demand, supply, and the costs of procurement and transportation are considered. Additionally, the model features three objectives: shortening the travel time, reducing the goods shortage, and saving the total cost of pre- and post-disaster phases. In order to handle the uncertainties, the robust optimization approach is utilized. The numerical example is solved with ε-constraint exact method, and this case illustrates the specific process of goods distribution, the relationship between objectives, and the sensitivity analysis of uncertainties. For the large-size forms, two heuristic algorithms are proposed and the efficiency of the proposed algorithms is assessed.

INDEX TERMS Emergent phenomena, resource management, Pareto optimization, uncertainty, heuristic algorithms.

I. INTRODUCTION

In recent years, natural disasters such as earthquakes, floods, lightning, fires, and etc. have gradually become the main cause of massive power outages [1]. For example, in January 2008, there was continuous snow weather in southern China, resulting in a power outage affecting about 110 million people and a direct economic loss of 151.65 billion RMB yuan. However, destructive effects of disruptions in the power supply, although inevitable, can be decreased by a proactive approach and development of appropriate preparation plans. Therefore, an effective relief approach is necessary, for ensuring the timely supply of grid emergency goods, restoring the smooth flow of transmission lines and the normal operation of the power grid as soon as possible.

At present, State Grid Corporation of China (SGCC) adopts a unified procurement and hierarchical management strategy, with the principle that the rescue order is from the near to the distant and the goods are purchased after utilizing up inventories. However, the total rescue time and the total cost cannot reach optimal values because the transportation route is not planned. Meanwhile, compared with the projects in the main grid and distribution network, the comprehensive plan for emergency rescue is affected deeply by environment and weather. Due to the insufficient depth of predictions about natural disasters, parameters such as goods demand and transportation cost have strong uncertainties. However, they are currently estimated based on operational experience.

In addition, in the phase of goods supply for disaster relief, the lack of effective connection between on-site demand and goods supply potentially gives rise to panic orders and a surge in non-tendering orders, resulting in inventory backlog and slow settlement of suppliers. Consequently, the unified centralized procurement method and traditional experience-based distribution plan in SGCC have been unable to handle the growing types and quantities of grid emergency goods. In view of the differences in the transportation costs, supply

environment and goods demand, it is urgent to research the procurement and distribution strategies of emergency goods.

Accordingly, this paper proposes an optimization model to address post-disaster transportation and distribution issues with respect to affected areas (AAs). The unpredictable stochastic essence of natural disasters, which is the topic of this study, requires a thorough design for simulating the real situation after the occurrence. Therefore, we consider the logistics uncertainties in demand, supply, and the costs of procurement and transportation.

Meanwhile, a three-level relief chain consisting of suppliers, relief distribution centers (RDCs), and AAs is considered in our model, with a focus on determining the relief goods flow and effective information exchange. In order to deliver relief goods to AAs within the least possible time, the optimum location and capacity of RDCs can be estimated in pre-disaster phase, such that the necessary goods can be stored beforehand. To better understand the gap and the contribution of our paper, a concise literature review is presented in the following.

II. LITERATURE REVIEW

In the research of grid emergency rescue, scholars utilize practical experience and establish some technical systems for disaster alleviation and prevention. Wang *et al.* [2] and Arab *et al.* [3] explored ways to prepare and harden the grid, and increased the resilience of the power grid under natural disasters. Liu and Singh [4] built a fuzzy inference system to assess how adverse weather affects the reliability parameters of system components. Panteli *et al.* [5] built a fragility model of individual components and the whole transmission system for mapping the real-time impact of severe weather, and assessed the spatiotemporal impact of a windstorm moving across a transmission network. Espinoza *et al.* [6] presented a multi-phase resilience assessment framework to analyze the continuous impact on critical infrastructures, then discussed different strategies to enhance the resilience of the electricity network. The researches pay more attention to enhancing resilience and increasing faster restoration of the grid system by advanced smart grid technologies.

The other direction mainly focuses on facility location, network flow, and inventory management based on electrical characteristics sometimes. Luo *et al.* [7] estimated the degree of blackouts and formulated a differentiated deployment strategy for important blackout areas. Bian and Fang [8] proposed a location model of power emergency goods storage considering load rating. Mete and Zabinsky [9] used a stochastic optimization method to determine the inventory level of goods. Zhang [10] and Sheu [11] predicted goods demand for satisfying relief requirements with intelligent algorithms. In order to assess the electrical characteristics of different AAs, Doorman et al. [12] developed a comprehensive methodology for analyzing grid vulnerability with respect to the energy shortage, capacity limitations, and other failures; Fang *et al.* [13] proposed a maximum flow-based complex network approach to identify the critical lines in the power grid.

On the other hand, the uncertainty is an inseparable part of emergency goods distribution [14]–[16]. For example, when a disaster occurs, the unknown extent of goods availability and the unpredictability of suppliers' contributions lead to the uncertainty of supply parameters [17]. The uncertainty in costs originates from the accessibility of transportation routes. The volatility and inaccurate estimation lead to the uncertainty in demand. Totally speaking, uncertain parameters can significantly increase the complexity of goods distribution, turning it into an optimization problem under uncertainty. Thus, Bozorgi *et al.* [18] proposed a robust programming model to simulate uncertain variables in disaster relief through multi-scenario partitioning. Tofighi *et al.* [19] presented a two-stage stochastic fuzzy model for pre-disaster phase and emergency resource distribution phase. Murali *et al.* [20] formulated a special case of the maximal covering location problem and accounted for demand which is distance-sensitive.

According to the conducting literature review, the uncertainty is mainly handled by stochastic programming. However, it usually requires advance knowledge about the probability distributions of uncertain parameters, which is difficult to accurately identify because of insufficient historical data in many real cases. In this article, we apply scenario-based robust programming instead, which uses a set of distinct scenarios to simulate the uncertainties. For the small-size problems, we solve the problem using an exact method called the ε-constraint method. For the large-size instances, for avoiding the computational challenges that may be introduced due to large number of scenarios, near-optimal solution approaches such as heuristic algorithms are utilized.

However, there are still some deficiencies in the relevant literatures on the topic of this article. Firstly, the literatures about grid relief logistics show that models combining the time and cost aspects have been explored far less than the single-objective models. Secondly, the just distribution and response to demands are also important subjects that have not been explored in the literatures. Thirdly, most researchers have assumed that all parameters are certain, which, with respect to the real world limitations, especially in the field of grid emergency logistics, are uncertain. Finally, the majority of researches in this field have concentrated on enhancing resilience and increasing faster restoration of the power grid. In terms of goods distribution, further development is needed.

Therefore, this article tackles the grid emergency goods distribution problem as a multi-objective, mixed-integer model under uncertainty. The contribution of this paper can be explained as follows. (1) Considering the importance of AAs based on electrical characteristics, the concept of distribution priority is proposed and considered as one of the constraints in the multi-objective optimization model. (2) Considering the real scenario of grid emergency rescue, the model takes the minimum total time as the core objective, and considers the minimum goods shortage, the

minimum total cost as the secondary objectives. To the best of our knowledge, simultaneous combination of them is not reported yet. (3) This article analyzes the impact of uncertain parameters (demand/supply/cost) on the above three objectives and makes a sensitivity analysis on different degrees of uncertainty. (4) To solve the multi-objective model, an exact method (ε-constraint method) and two heuristic algorithms (MOPSO/NSGA-II) are proposed and some comparisons are made.

The remainder of this article is organized as follows. In Section 3, the priority of emergency logistics is determined according to the electrical importance of AAs. In section 4, the robust optimization approach to describe uncertain parameters, the mathematical model to distribute goods, and the algorithms to solve the multi-objective optimization problem are presented. Section 5 provides a numerical example, illustrating the effect of uncertain parameters and the comparisons of different intelligent algorithms. Finally, the conclusions and future research directions are expressed in Section 6.

III. DISTRIBUTION PRIORITY FOR AAS

According to the complex network theory [21], the power grid can be regarded as a complex network composed of nodes V (power plants, substations, and loads) and connecting lines E (transmission lines and transformer branches) between nodes. We classify a node and the 1/2 range of each connecting line as a network node. If a network node exists power equipment, roads, and other resources that are damaged by natural disasters, then the network node is defined as an AA.

In order to determine the rescue sequence to AAs, it is necessary to assess the importance of AAs. Therefore, we utilize the network condensation degree to characterize the importance of the network node and its associated lines, and adopt the power betweenness [22], [23] to characterize the electrical performance of generators and loads in the network node, aiming at assessing the importance comprehensively.

A. NETWORK CONDENSATION DEGREE

Network contraction is to contract all nodes connecting to a node and condense into a new node. The contraction process is shown in Figure 1.

The network condensation degree A after contraction is shown in (1).

$$\begin{cases} A = 1/nl \\ l = \sum\limits_{i \neq j \in V} E_{ij}/n\,(n-1) \end{cases} \tag{1}$$

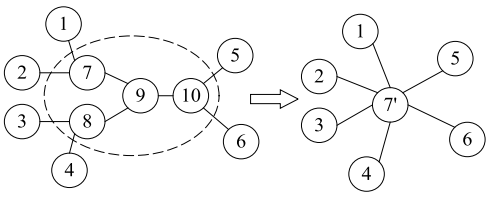

FIGURE 1. Demonstration of node contraction.

where, n is the node number in the entire network system, E_{ij} is the transmission betweenness between nodes i and j, l is the average of the shortest lengths between two nodes. Meanwhile, E_{ij} is defined as the average of the sum of the line betweenness B_{ij} and the total transfer capacity P_{ttc_ij}, i.e.$E_{ij} = \left(B_{ij} + P_{ttc_ij}\right)/2$, and E_{ij} can describe the physical and electrical characteristics of transmission lines.

The line betweenness B indicates the degree of intermediary function that a line takes on in the network, and it is defined as (2).

$$\begin{cases} B_{k.ij} = \sum\limits_{i \neq j \in V} N_{ij}\,(k) / \sum\limits_{i \neq j \in V} N_{ij} \\ B_{ij} = \sum\limits_{k \in K} B_{k.ij} \end{cases} \tag{2}$$

where, $B_{k.ij}$ is the betweenness of the transmission line k between nodes i and j; V is a set of all nodes; $\sum\limits_{i \neq j \in V} N_{ij}\,(k)$ is the frequency that line k is considered as the shortest route; $\sum\limits_{i \neq j \in V} N_{ij}$ is the frequency that all lines between nodes i and j are considered as the shortest route, K is a set of all routes between nodes i and j.

The total transfer capacity P_{ttc_ij} is the maximum power that the transmission line between nodes i and j can withstand under normal working conditions. Generally, it is controlled by the power dispatching department.

B. THE POWER BETWEENNESS OF NODES

The importance assessment of AAs should not only consider the network node and its associated transmission lines, but also analyze the electrical performance of generators and loads. The performance can be expressed by the power betweenness D_i, which is:

$$D_i = W_i \left(\omega_G \cdot \frac{n_G}{n} \cdot \sum_{k=1}^{n_G} P_{Gik} + \omega_L \cdot \frac{n_L}{n} \cdot \sum_{k=1}^{n_L} P_{Lik} \right) \tag{3}$$

where, D_i is the power betweenness of node i; n is the number of nodes; ω_G and ω_L are the weight coefficients of generators and loads in node i, respectively; n_G and n_L are the number of generators and loads contained in node i, respectively; P_{Gik} and P_{Lik} are the active power of the k^{th} generator and the k^{th} load in node i, respectively; W_i is the transmission power coefficient of node i.

C. THE INDICATOR FOR COMPREHENSIVE ASSESSMENT

Due to the different magnitude of each indicator, making the data more difficult to handle. Therefore, it is necessary to normalize different indicators. The normalization method is shown in (4).

$$\begin{aligned} A^* &= (A - A_{\min})/(A_{\max} - A_{\min}) \\ B^* &= (B - B_{\min})/(B_{\max} - B_{\min}) \\ P^* &= (P_{\max} - P)/(P_{\max} - P_{\min}) \\ D^* &= (D - D_{\min})/(D_{\max} - D_{\min}) \end{aligned} \tag{4}$$

Combining the commonality of complex networks with the characteristics of electrical networks, the importance assessment indicator U can be defined as (5). With the value of U increasing, the importance of AAs becomes higher; and vice versa.

$$U = \left(A^* + D^*\right)/2 \tag{5}$$

IV. MODEL DESCRIPTION

Due to the unpredictability of natural disasters, the demand, supply, and cost of emergency goods are all considered as uncertain parameters in our approach. Therefore, this paper captures uncertainty based on robust optimization, in which uncertainty is represented by a set of discrete scenarios [24], [25], and we presents a multi-objective, mixed-integer, nonlinear programming model.

The premise of our multi-objective optimization model is that emergency goods must be given priority to the AA with the highest value $U_{\max}$. Meanwhile, the model considers three objectives: the first objective function Obj_1 is to minimize total time, and this is the core objective; the second objective function Obj_2 is to minimize goods shortage; the third objective function Obj_3 is to minimize total cost, Obj_2 and Obj_3 are considered as the secondary objectives.

A. OBJECTIVE FUNCTIONS

The relief distribution process is shown in Figure 2. RDCs are hubs that connect suppliers and AAs, and are responsible for collecting and allocating emergency goods. When constructing an emergency response network, the location of RDCs needs to be completed. The selection factors are (1), the storage capacity of RDCs; (2), the distance to AAs. In order to reduce transportation costs and distribute more efficiently, RDCs can be positioned close to both suppliers and AAs. Meanwhile, the approach consists of two basic phases. The first phase (i.e. pre-disaster phase) determines the optimal location of RDCs and the inventory of relief goods stored by suppliers; the second phase (i.e. post-disaster phase) determines the quantity of relief goods transferred from supplies to RDCs, and from RDCs to AAs.

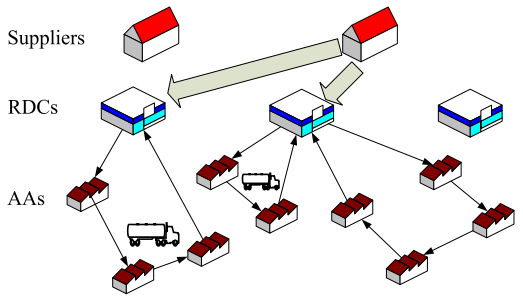

FIGURE 2. The relief distribution process.

In order to define Obj_1-Obj_3, we introduce some parameters shown in Table 1.

TABLE 1. Parameters and their signification.

Symbol	Signification
I	set of suppliers i, $i \in I$
J	set of candidate RDCs j, $j \in J$
K	set of AAs k, $k \in K$
S	set of goods types s, $s \in S$
P	set of possible scenarios p, $p \in P$
F_j	fixed establishing cost of RDC j
b_{si}	unit procurement cost of goods s from supplier i
C_{si}	quantity of goods s that can be provided from supplier i
t_{psij}	unit transportation cost of goods s from supplier i to RDC j under scenario p
t_{psjk}	unit transportation cost of goods s from RDC j to AA k under scenario p
p_{sk}	unit inventory shortage cost for goods s at AA k
q_{sk}	unit inventory holding cost for goods s at AA k
v_s	unit required area of goods s
V_j	maximum capacity of an established RDC j
X_j	1 if RDC is located at candidate RDC j ;0 otherwise
x_{sij}	quantity of goods s procured from supplier i and stored at RDC j
x_{psij}	quantity of goods s transferred from supplier i to RDC j under scenario p
y_{psjk}	quantity of goods s transferred from RDC j to AA k under scenario p
d_{psk}	demand quantity of goods s at AA k under scenario p
z_{psk}	shortage quantity of goods s at AA k under scenario p
r_{psk}	remaining quantity of goods s at AA k under scenario p
T_{pij}	maximum time from supplier i to RDC j under scenario p
T_{pjk}	maximum time from RDC j to AA k under scenario p

In Table 1, demand, supply and the costs of procurement and transportation are uncertain and related to a specific scenario p. Here, the scenario p can be considered as a random event. Based on the robust optimization led by Mulevy *et al.* [26], we uses a set of distinct scenarios to simulate the uncertainties, consequently the objective function under the scenario p is:

$$\min \sum_{p\in P} p_p \xi_p + \lambda \sum_{p\in P} p_p \left[\left(\xi_p - \sum_{p'\in P} p_{p'} \xi_{p'} \right) + 2\theta_p \right] + \gamma \sum_{p\in P} p_p \delta_p \tag{6}$$

$$\text{s.t. } \xi_p - \sum_{p\in P} p_p \xi_p + \theta_p \geq 0 \tag{7}$$

where, ξ is a custom function; error vector δ_p indicates the infeasibility under scenario p because of uncertain parameters; γ is the infeasibility penalty coefficient; λ is the variability weight (i.e. uncertainty degree); p_p is the occurrence probability of scenario p; variable θ can be interpreted as the amount by which $\xi_p > \sum_{p\in P} p_p \xi_p$, then $\theta_p = 0$, while as the amount by which $\xi_p < \sum_{p\in P} p_p \xi_p$, then $\theta_p = \sum_{p\in P} p_p \xi_p - \xi_p$.

Therefore, the first objective function Obj_1 that minimizes total time is formulated as (8):

$$\begin{aligned}\min Obj_1 &= \sum_{p\in P} p_p \cdot \left(\sum_{i\in I}\sum_{j\in J} T_{pij} + \sum_{k\in K}\sum_{j\in J} T_{pjk}\right) \\ &+\lambda_1 \cdot \sum_{p\in P} p_p \cdot \left[\left(\sum_{i\in I}\sum_{j\in J} T_{pij} + \sum_{k\in K}\sum_{j\in J} T_{pjk}\right) - \sum_{p'\in P} p_{p'} \right. \\ &\left. \cdot \left(\sum_{i\in I}\sum_{j\in J} T_{p'ij} + \sum_{k\in K}\sum_{j\in J} T_{p'jk}\right) + 2\theta_{1p}\right]\end{aligned} \tag{8}$$

The second objective function Obj_2 that minimizes goods shortage is formulated as (9):

$$\begin{aligned}\min Obj_2 &= \sum_{p\in P} p_p \cdot \left(\sum_{s\in S} \max_{k\in K}\left\{s_{psk}\right\}\right) \\ &+\lambda_2 \cdot \sum_{p\in P} p_p \cdot \left[\left(\sum_{s\in S} \max_{k\in K}\left\{s_{psk}\right\} - \sum_{p'\in P} p_{p'}\right.\right. \\ &\left.\left. \cdot \sum_{s\in S} \max_{k\in K}\left\{s_{p'sk}\right\}\right) + 2\theta_{2p}\right]\end{aligned} \tag{9}$$

where, s_{psk} is the shortage ratio of goods s at AA k under scenario p, $s_{psk} / \left(\sum_{j\in J} y_{psjk} + z_{psk}\right)$.

The third objective function Obj_3 that minimizes total cost is formulated as (10):

$$\begin{aligned}\min Obj_3 &= SC + PC + \sum_{p\in P} p_p \left(TC_{1p} + TC_{2p} + PC_p + QC_p\right) + \lambda_3 \\ &\cdot \sum_{p\in P} p_p \left[\left(TC_{1p} + TC_{2p} + PC_p + QC_p\right) - \sum_{p'\in P}\right. \\ &\left. p_{p'}\left(TC_{1p'} + TC_{2p'} + PC_{p'} + QC_{p'}\right) + 2\theta_{3p}\right] \\ &+\gamma \sum_{j\in J}\sum_{s\in S}\sum_{p\in P} p_p \delta_{jsp}\end{aligned} \tag{10}$$

where, SC is the setup costs of RDCs; PC is the procurement cost in pre-disaster phase; TC_{1p} is the transportation cost from suppliers to RDCs in post-disaster phase; TC_{2p} is the transportation cost from RDCs to AAs in post-disaster phase; PC_p is the shortage cost in AAs; QC_p is the inventory holding cost in AAs. Their expressions are as (11).

$$\begin{aligned} SC &= \sum_{j\in J} F_j X_j \\ PC &= \sum_{i\in I}\sum_{j\in J}\sum_{s\in S} b_{si} x_{sij} \\ TC_{1p} &= \sum_{i\in I}\sum_{j\in J}\sum_{s\in S} t_{psij} x_{psij} \\ TC_{2p} &= \sum_{j\in J}\sum_{k\in K}\sum_{s\in S} t_{psjk} y_{psjk} \\ PC_p &= \sum_{k\in K}\sum_{s\in S} p_{sk} z_{psk} \\ QC_p &= \sum_{k\in K}\sum_{s\in S} q_{sk} r_{psk} \end{aligned} \tag{11}$$

The constraints can be expressed as (12)-(22).

$$\sum_{j\in J} x_{sij} \le C_{si} \forall s \in S, i \in I \tag{12}$$

$$\sum_{i\in I}\sum_{s\in S} v_s x_{sij} \le V_j X_j \quad \forall j \in J \tag{13}$$

$$\sum_{k\in K}\sum_{p\in P}\sum_{s\in S} v_s \cdot y_{psjk} \le V_j \cdot X_j \quad \forall j \in J \tag{14}$$

$$\sum_{p\in P}\sum_{k\in K} y_{psjk} \le \sum_{i\in I} x_{sij} \quad \forall s \in S,\ \forall j \in J \tag{15}$$

$$\begin{aligned}\sum_{i\in I} x_{psij} + \sum_{i\in I} x_{sij} + \left(\sum_{k\ne j\in J} y_{psjk}\right)\left(X_j - 1\right) \\ = \delta_{jsp} \quad \forall j \in J, s \in S, p \in P\end{aligned} \tag{16}$$

$$\sum_{j\in J} y_{psjk} + z_{psk} - r_{psk} = d_{psk} + \delta_{psk} \quad \forall s \in S,\ \forall k \in K \tag{17}$$

$$\begin{aligned}&\left(\sum_{i\in I}\sum_{j\in J} T_{pij} + \sum_{k\in K}\sum_{j\in J} T_{pjk}\right) \\ &- \sum_{p'\in P} p_{p'} \cdot \left(\sum_{i\in I}\sum_{j\in J} T_{p'ij} + \sum_{k\in K}\sum_{j\in J} T_{p'jk}\right) \\ &+ \theta_{1p} \ge 0 \quad \forall p \in P\end{aligned} \tag{18}$$

$$\begin{aligned}&\sum_{s\in S} \max_{k\in K}\left\{s_{psk}\right\} - \sum_{p'\in P} p_{p'} \\ &\cdot \sum_{s\in S} \max_{k\in K}\left\{s_{p'sk}\right\} + \theta_{2p} \ge 0 \quad \forall p \in P\end{aligned} \tag{19}$$

$$\begin{aligned}&\left(TC_{1p} + TC_{2p} + PC_p + QC_p\right) \\ &- \sum_{p'\in P} p_{p'} \cdot \left(TC_{1p'} + TC_{2p'} + PC_{p'} + QC_{p'}\right) \\ &+ \theta_{3p} \ge 0 \quad \forall p \in P\end{aligned} \tag{20}$$

$$s_{ps1} > s_{ps2} > \cdots > s_{psk} \quad \forall k \in K, U_1 < U_2 < \cdots < U_k \tag{21}$$

$$\begin{aligned}&X_j \in \{0, 1\}\, x_{sij}, x_{psij}, y_{psjk}, \\ &d_{psk}, z_{psk}, r_{psk}, \delta_{jsp}, \theta_{1p}, \theta_{2p}, \theta_{3p} \ge 0\end{aligned} \tag{22}$$

where, (12) is the total distribution goods constraint of suppliers; (13) and (14) are the distribution goods capacity constraints of RDCs; (15) is the total distribution goods constraint of RDCs; (16) is the total goods demand constraint of RDCs; (17) is the total goods demand constraint of AAs; (18), (19), and (20) are auxiliary constraints for linearization defined in (8); (21) is the condition that emergency goods must be given priority to AAs depending on the importance indicator U.

(22) is an integer constraint and a non-negative constraint of parameters.

B. SOLUTION APPROACH

Multi-objective optimization is the process that optimizes three conflicting objectives while taking a series of constraints into account. Thus the model of this paper can be described as (23).

$$\begin{cases} \min\ F(x) = \{f_1(x), f_2(x), f_3(x)\} \\ \text{s.t. } h(x) = 0, \quad g(x) \le 0 \end{cases} \tag{23}$$

where, $f(x)$ is the objective function; $h(x)$ is the equality constraint function; $g(x)$ is the inequality constraint function.

1) ε-CONSTRAINT EXACT METHOD

Due to the conflict existing among three objectives, no single solution can be found that optimizes all objectives. Therefore, the concept of non-dominant solutions or Pareto solutions is brought up. In low dimension problems, there are several common methods converting several objectives into one objective and obtaining exact solutions, such as: weighted sum, ε-constraint method, and min-max approach. Currently, the weighted sum is the most commonly used approach [27]. However, the method can only generate extreme efficient solutions, and it is highly dependent on the assigned weights, which is difficult to calculate accurately. In contrast, ε-constraint method is able to generate non-extreme efficient solutions, and it can control the number of generated solutions by adjusting the preferred break-points [28]. Therefore, we handle the multi-objective problem by ε-constraint method.

As mentioned before, the first objective is considered as the core objective and the rest are secondary objectives. Therefore the formulation is as in (24), Obj_1 is optimized while Obj_2 and Obj_3 are added to constraints.

$$\begin{cases} \min\ Obj_1 \\ \text{s.t. } Obj_2 \le \varepsilon_2, Obj_3 \le \varepsilon_3 \end{cases} \tag{24}$$

2) HEURISTIC ALGORITHM

In low dimension problem, an exact method called ε-constraint above is utilized. However, exact methods are not proper for large-size problems. Therefore, heuristic algorithms have been gradually applied to multi-objective large-size optimization problems.

The non-dominated sorting genetic algorithm (NSGA-II) [29] is one of the most commonly used optimization algorithms in the multi-objective optimization problems [30] and has been used as a base to test the performance of other algorithms [31]. Meanwhile, the multi-objective particle swarm optimization (MOPSO) algorithm is widely used [32]. Thus, NSGA-II and MOPSO are utilized in this article. The specific analysis is in Section 5.4.

Figures 3–4 explain the solution process of MOPSO and NSGA-II, considering a case with five suppliers (I), four candidate RDCs (J), and six AAs (K).

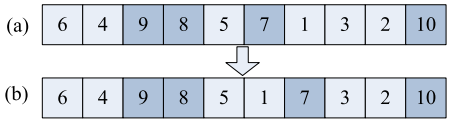

FIGURE 3. The original and revised chromosomes of AAs and RDCs.

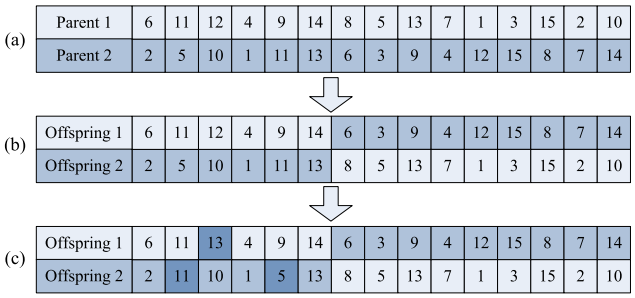

FIGURE 4. Offspring chromosomes after crossover and mutation.

In the chromosome in Figure 3(a), numbers 1 to 6 indicate AAs and numbers 7 to 10 indicate candidate RDCs. Therefore, 1 AA to the first RDC, 0 AA to the second RDC, 2 AAs to the third RDC, 3 AAs to the fourth RDC, are allocated. Not allocating an AA to a RDC means that the RDC is not set up. However, it is necessary to confirm the capacity constraint of RDCs. In any case, if the allocated quantities from a RDC exceed its capacity, the last AA allocated to its RDC is transferred to the next RDC. For example, the total demand quantities of AAs 1, 2, and 3 exceed the capacity of the fourth RDC 10. Therefore, AA 1 need to be allocated to the first RDC 7, shown in Figure 3(b). Supplier and RDC chromosomes are defined similarly.

Figure 4 is the offspring chromosomes after crossover and mutation process. Supposing crossover probability Pc=0.6, thus the crossover chromosomes=9; mutation probability Pm=0.1, thus the mutation chromosomes=3. Numbers 1 to 15 represent all suppliers, candidate RDCs, and AAs. Figure 4(a) is the parent chromosomes originally. After crossover, there are nine chromosomes have been changed, and the offspring chromosomes are shown in Figure 4(b). And Figure 4(c) shows the offspring chromosomes after mutation. Numbers 5, 11, 13 are the mutated chromosomes.

3) PARAMETER TUNING

It is necessary to set suitable parameters of heuristic algorithms. Taguchi method is one of the most efficient methods for setting parameters, and it minimizes the changes and sensitivity of chaos factors [33]. NSGA-II parameters include population size (Ns), crossover possibility (Pc), mutation possibility (Pm), and maximum number of iterations (Max-it), and MOPSO parameters include Ns, Max-it, personal learning coefficient (C_1), and global learning coefficient (C_2).

Table 2 shows different levels of parameters and Figures 5–6 show the related S/N ratios obtained by the Minitab software. The one with the highest S/N ratio is selected as the best parameters.

TABLE 2. The parameters of the algorithms and their levels.

Algorithm	Parameters	Level		
		Low(1)	Medium(2)	High(3)
NSGA-II	Ns	50	70	90
	Pc	0.7	0.8	0.9
	Pm	0.1	0.2	0.4
	Max-it	100	200	300
MOPSO	Ns	80	90	100
	C_1	1	1.5	2
	C_2	1	1.5	2
	Max-it	100	200	300

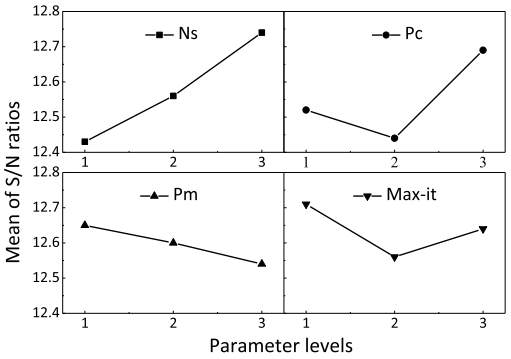

FIGURE 5. The S/N ratios of NSGA-II parameters.

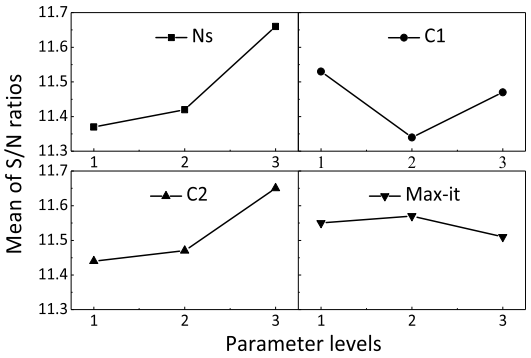

FIGURE 6. The S/N ratios of MOPSO parameters.

V. CASE ANALYSIS

The real-world case lies in Sichuan Province, China (Figure 7), and it suffered from an earthquake disaster. Figure 7(a) shows the location of two suppliers and three AAs in reality, meanwhile, the corresponding network topology considering transmission lines is shown in Figure 7(b). Additionally, the two suppliers are named of S1, S2, and the three AAs are named of D1, D2, and D3.

A. PRIORITIZATION OF GOODS DISTRIBUTION FOR AAS

Since the total transfer capacity and the line betweenness respectively represent different attributes of transmission lines, there are different values shown in Figure 8.

Table 3 shows that $U_{xD3} > U_{xD2} > U_{xD1}$. Therefore, the priority of goods distribution to AAs is: D3>D2>D1.

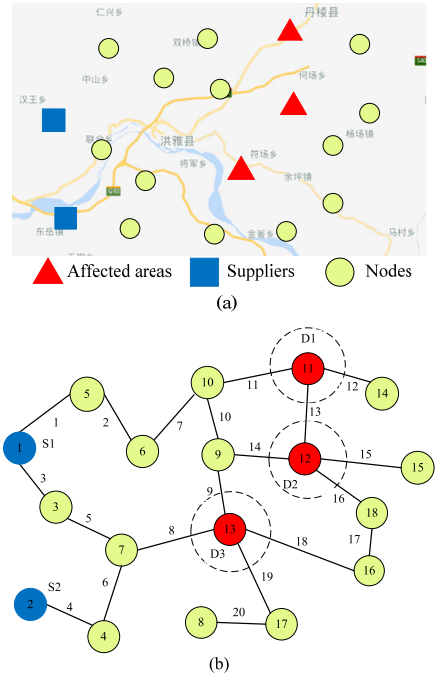

FIGURE 7. The map and corresponding network topology of the sample problem.

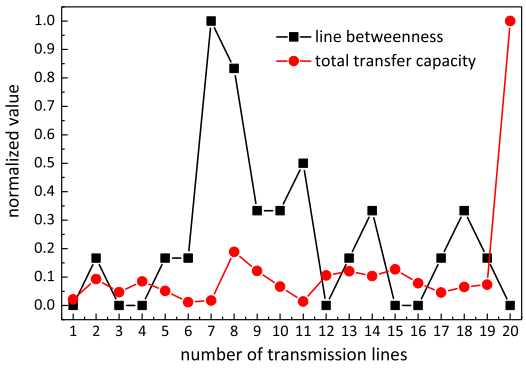

FIGURE 8. Normalized values of line betweenness (B) and total transfer capacity (P_{ttc}) of each line in the AAs.

TABLE 3. Calculation results of importance indicators (U_x) of AAs.

AAs	A_x^*	D_x^*	U_x	Priority ordering
D1	0.2358	0.0000	0.1179	3
D2	0.0000	1.0000	0.5000	2
D3	1.0000	0.3333	0.6667	1

B. SPECIFIC DISTRIBUTION PROCESS

In dealing with disasters, three types of emergency goods named of R1, R2, and R3 are considered in this case, including rescue vehicles, rescue tools, etc. We also consider four scenarios simultaneously: P1, P2, P3, and P4, with occurrence probabilities of 0.45, 0.3, 0.1, and 0.15, respectively. These scenarios and associated probabilities are designed by disaster planners based on historical records and known geological faults [18]. The variability weight λ_i is equal to

TABLE 4. The ability of each supplier to provide goods.

Suppliers	R1(P1,P2,P3,P4)	R2(P1,P2,P3,P4)	R3(P1,P2,P3,P4)
S1	(675,450,150,225)	(405,270,90,135)	(360,240,80,120)
S2	(450,300,100,150)	(315,210,70,105)	(270,180,60,90)

TABLE 5. Fixed establishing cost of a RDC depending on its storage capacity.

Size	Cost $F_j(10^2$ ¥)	Capacity (10^2 m^3)
Small	50	10
Medium	80	16
Large	120	24

TABLE 6. Unit procurement cost, goods volume, and transportation cost.

Category	$b_{si}(10^2$ ¥)	v_s(m^3)	$t_{psij}(10^2$ ¥)	$t_{psjk}(10^2$ ¥)
R1	0.5	1.5	0.3	0.54
R2	2	2	0.08	0.15
R3	20	4.5	0.9	1.62

TABLE 7. Demand for each AA in four scenarios.

Category	D1(P1,P2,P3,P4)	D2(P1,P2,P3,P4)	D3(P1,P2,P3,P4)
R1	(68,169,158,113)	(0,103,81,76)	(0,22,75,22)
R2	(68,169,158,113)	(0,103,81,76)	(0,22,75,22)
R3	(23,56,53,38)	(0,34,27,25)	(0,7,25,7)

TABLE 8. The inventory quantity of goods in RDCs in pre-disaster phase (x_{sij}).

RDC	Size	R1	R2	R3
RDC1	Large	460	320	150
RDC2	Small	—	—	40
RDC3	Small	—	—	—
RDC4	Medium	—	182	209

0.5 for $i \in I$. Table 4-7 show the data collected in pre-disaster phase.

Table 7 shows that for each AA, there is a four-element vector that represents goods demands under different scenarios. Demand is estimated on the basis of the power equipment density multiplied with the importance indicator U.

Table 8 shows that there are four RDCs in pre-disaster phase: one RDC stores only one goods (R3); one RDC stores only two goods (R2, R3); one RDC stores all three types of goods; one RDC stores nothing. The "-" in Table 8 means no storage. Formulating $T_{pij} = 1.5$h, $T_{pjk} = 2$h, then we solve the small-size problem using GAMS software by ε-constraint method. The results are shown in Tables 9–10.

Taking the data in Table 9 as an example, RDC1 receives 95 units and 57 units R3 from S1 and S2 suppliers under the fourth scenario (P4). The "-" in Table 9 means no distribution.

TABLE 9. The quantity transferred from suppliers to RDCs under different scenarios in post-disaster phase (x_{psij}).

Suppliers	Category	RDC1(P1-P4)	RDC2(P1-P4)	RDC3(P1-P4)	RDC4(P1-P4)
S1	R1	—	(27,0,0,0)	—	(140,25,124,0)
	R2	—	—	—	—
	R3	(0,0,0,95)	(0,0,65,0)	—	—
S2	R1	—	(0,0,69,23)	—	—
	R2	—	—	(0,10,117,0)	—
	R3	(0,0,0,57)	—	(0,121,0,0)	—

TABLE 10. The quantity transferred from RDCs to AAs under different scenarios in post-disaster phase (y_{psjk}).

RDC	Category	D1(P1-P4)	D2(P1-P4)	D3(P1-P4)
RDC1	R1	(0,80,0,40)	(11,11,10,0)	(40,24,8,12)
	R2	(51,34,11,17)	(34,41,0,0)	(15,10,0,5)
	R3	(10,7,3,5)	(28,19,7,10)	—
RDC2	R1	(7,0,0,0)	—	(0,0,49,0)
	R2	—	—	—
	R3	(0,0,32,0)	(0,0,35,0)	—
RDC3	R1	—	—	—
	R2	—	—	(0,0,68,0)
	R3	—	(0,14,0,0)	—
RDC4	R1	(42,21,7,0)	—	(29,0,0,0)
	R2	—	(37,32,0,13)	(0,0,0,24)
	R3	(42,28,9,13)	(0,0,28,20)	—

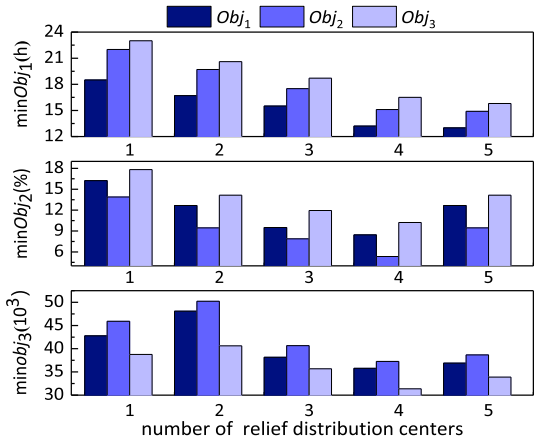

FIGURE 9. Optimal solutions of the objective functions (independently solved).

In Table 10, when the quantity of the RDC closest to an AA is in short supply, the second RDC closest to the AA provides goods. The "-" in Table 10 means no distribution.

In order to determine the number j of RDCs, optimal values of objective functions can be obtained by varying possible number j. Figure 9 depicts the values of min Obj_1, min Obj_2, and min Obj_3 while $j = 1, 2, 3, 4, 5$. When $j = 4$, min Obj_1, min Obj_2, and min Obj_3 all obtain the minimum values, so the optimal number j is assumed to be 4, and the number of RDCs in Table 8 is based on this assumption.

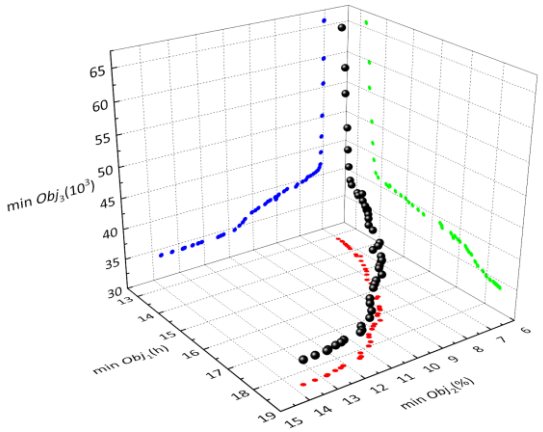

FIGURE 10. Three-dimension Pareto-optimal set.

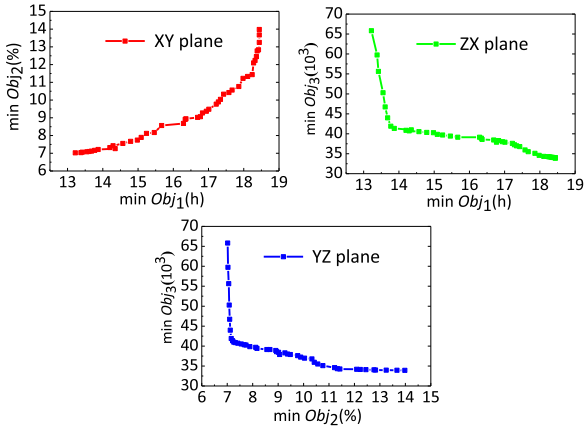

FIGURE 11. Projection diagram of the three-dimension Pareto-optimal set.

TABLE 11. Extreme solutions in Pareto-optimal set.

Objectives	Obj_1 (h)	Obj_2 (%)	Obj_3 (10^3 ¥)
Minimize Obj_1	13.22	7.02	65.81
Minimize Obj_2	13.22	7.02	65.81
Minimize Obj_3	18.46	13.98	33.88

Meanwhile, a widely distributed three-dimensional Pareto-optimal set is obtained, as shown in Figure 10. Figure 11 is the projections of the three-dimensional Pareto-optimal set on two-dimensional planes.

Figures 10–11 show that there is an association between three objective functions. Specifically, an increase in the total time (Obj_1) will result in an increase in the goods shortage (Obj_2) and a decrease in the total cost (Obj_3). Therefore, optimizing the total cost is at the expense of the other two objectives, and there is a positive correlation between the total time and the goods shortage.

If minimizing the total time (Obj_1), goods shortage (Obj_2), and total cost (Obj_3) are the objectives respectively to search extreme solutions, the results are shown in Table 11.

TABLE 12. Best compromise solutions in Pareto-optimal set.

Obj_1 (h)	Obj_2 (%)	Obj_3 (10^3 ¥)
13.77	7.12	41.89

Table 11 shows that, if only the total time or goods shortage is optimized, the economic burden of distribution will increase; if only the total cost is targeted, it will be unfavourable for the rapid supply of goods, so it is necessary to weigh all objectives and fully exploit the information in the Pareto-optimal set. The compromise solution is obtained from the Pareto-optimal set by the fuzzy membership function, shown in Table 12.

C. SENSITIVITY ANALYSIS OF UNCERTAINTIES

In order to quantitatively analyze the influence of uncertain parameters on disaster relief logistics planning, four typical models are compared according to different uncertain degrees of three parameters (demand/supply/cost). As shown in Table 13, the degree of uncertainty in models (M_1-M_4) is: $M_4 > M_3 > M_2 > M_1$. The uncertainty degree $\lambda = 0.5$.

Figure 12-14 show projections of Pareto-optimal sets on the XY, XZ, YZ plane. With the increasing degree of uncertainty, the optimal solution tends to increase total time, reduce shortage and total cost. The reasons are as follows.

M_1 does not consider uncertainty. Therefore an essential cost is incurred and causes total cost to become considerably unstable while dealing with different scenarios. When demand uncertainty is considered in M_2, the complexity of the model increases to some extent, resulting in a longer total time. However, the capability responding to unexpected situations improves as well, making a decrease

TABLE 13. Typical models with different degrees of uncertainty, M_4 is the model in this article.

Parameter	M_1	M_2	M_3	M_4
Demand	Certain	Uncertain	Uncertain	Uncertain
Supply	Certain	Certain	Uncertain	Uncertain
Cost	Certain	Certain	Certain	Uncertain

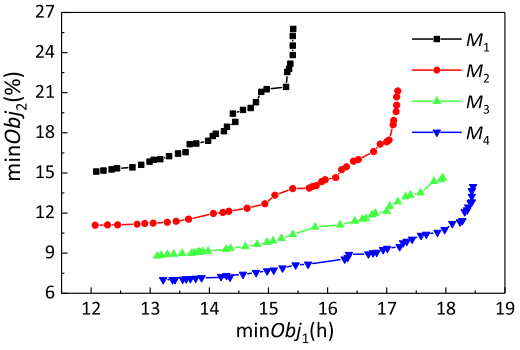

FIGURE 12. Pareto-optimal sets of typical models M_1-M_4 on the XY plane ($\lambda = 0.5$).

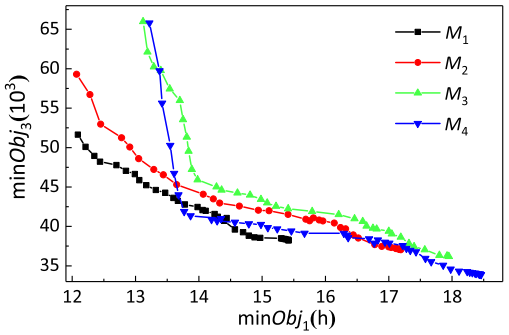

FIGURE 13. Pareto-optimal sets of typical models M_1-M_4 on the XZ plane ($\lambda = 0.5$).

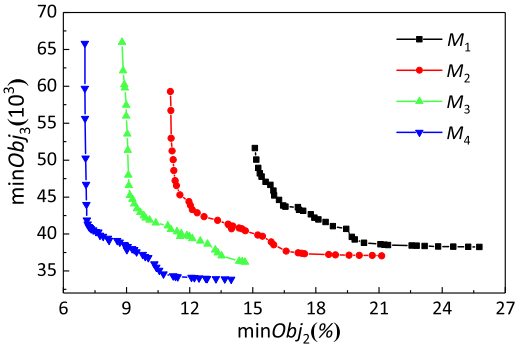

FIGURE 14. Pareto-optimal sets of typical models M_1-M_4 on the YZ plane ($\lambda = 0.5$).

TABLE 14. Pareto-compromised sets of models M_1-M_4.

Model	Obj_1 (h)	Obj_2 (%)	Obj_3 (10^3¥)
M_1	12.44	15.34	48.21
M_2	13.29	11.31	47.22
M_3	13.54	9.16	45.91
M_4	13.77	7.12	41.89

in goods shortage. Whenever higher degrees of uncertainty are considered, the complexity increases accordingly. However, the improvement in responsiveness reduces the cost of processing different scenarios, making a reduction in total cost.

In Table 14, models M_1, M_2, and M_3 have the results that the total time Obj_1 is 12.44h, 13.29h, and 13.54h; the goods shortage Obj_2 is 15.34%, 11.31%, and 9.16%; the total cost Obj_3 is 48.21 thousand RMB yuan, 47.22 thousand RMB yuan, and 45.91 thousand RMB yuan, respectively. In comparison with models M_1-M_3, which cover lower degrees of uncertainty, M_4 considering three sources of uncertainty increases the total time by 9.65%, 3.49%, and 1.67%; decreases the goods shortage by 8.22%, 4.19%, and 2.04%; and saves the total cost by 15.09%, 12.72%, and 9.60%, respectively. Figure 15 depicts the sensitivity analysis of the uncertainty level on the objective functions.

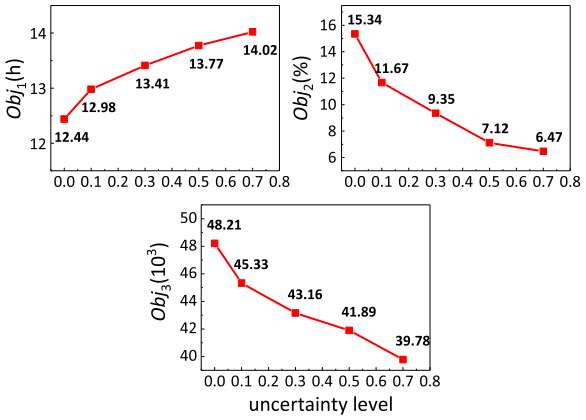

FIGURE 15. The correlation between objective functions and uncertainty level.

TABLE 15. General data of test problems.

Test No.	Size(I-J-K)	Test No.	Size(I-J-K)
1	3-3-2	6	12-13-17
2	3-4-7	7	15-18-20
3	5-4-10	8	17-21-24
4	6-7-11	9	25-30-34
5	9-6-9	10	30-35-42

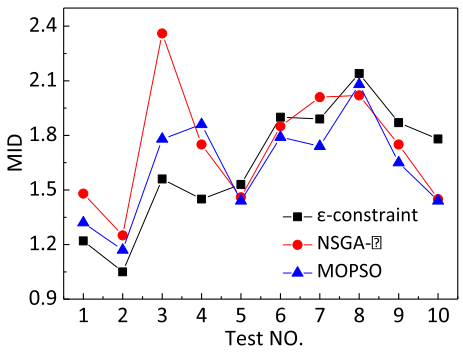

FIGURE 16. Comparison between the exact method and heuristic algorithms based on MID.

D. ANALYZING THE PERFORMANCE OF THE PROPOSED ALGORITHM

In order to compare the results of different algorithms, based on the works [34], [35], four criteria including mean ideal distance (MID), spacing metric (SM), diversification metric (DM), and calculation time (CPU time), are considered. MID shows the mean distance of the Pareto sets from origin, SM and DM show the distribution and diversification of the Pareto sets respectively, and CPU time is one of the most important criteria. Equations (25)–(27), shown at the top of next page, are definitions with the criteria.

where, c_i is the distance of the i^{th} Pareto point from the ideal, n is the number of Pareto sets, d_i is the Euclidean distance between two adjacent Pareto sets, $\bar{d}$ is the mean value of d_i, f_{1i}, f_{2i}, f_{3i} are the values of the i^{th} Pareto point for each objective functions.

$$\mathrm{MID} = \sum_{i=1}^{n} c_i / n \tag{25}$$

$$\mathrm{SM} = \left(\sum_{i=1}^{n} \left| \bar{d} - d_i \right| \right) / \left[(n-1)\, \bar{d} \right] \tag{26}$$

$$\mathrm{DM} = \sqrt{\left(\frac{\max f_{1i} - \min f_{1i}}{f_{1.total}^{\max} - f_{1.total}^{\min}} \right)^2 + \left(\frac{\max f_{2i} - \min f_{2i}}{f_{2.total}^{\max} - f_{2.total}^{\min}} \right)^2 + \left(\frac{\max f_{3i} - \min f_{3i}}{f_{3.total}^{\max} - f_{3.total}^{\min}} \right)^2} \tag{27}$$

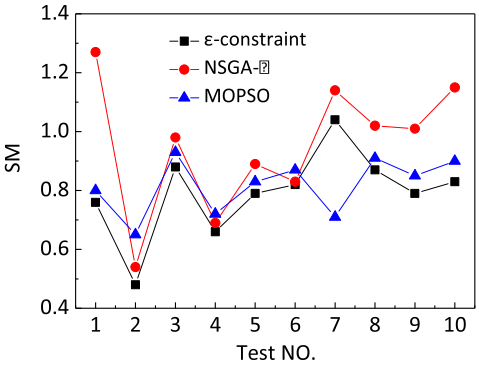

FIGURE 17. Comparison between the exact method and heuristic algorithms based on SM.

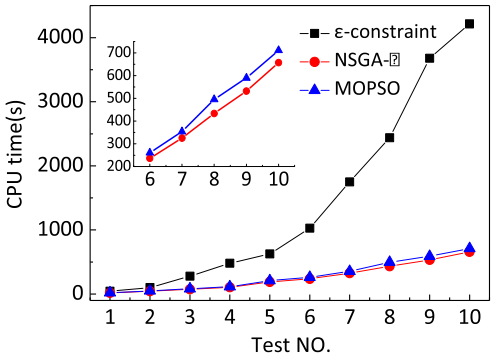

FIGURE 19. Comparison between the exact method and heuristic algorithms based on CPU time.

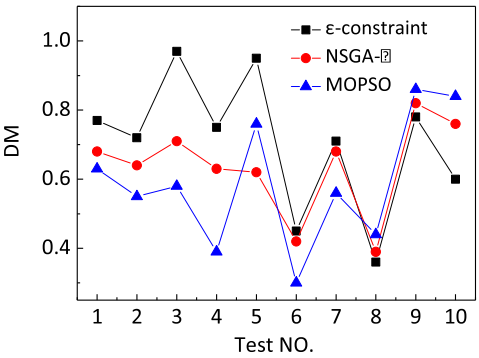

FIGURE 18. Comparison between the exact method and heuristic algorithms based on DM.

Thus, with the value of MID, SM, CPU time decreasing, the performance of algorithms is better; and with the value of DM increasing, the performance of algorithms is better. Figures 16-19 show the comparison between the exact method and heuristic algorithms.

In the low-dimension problems, the exact method performs closely compared to heuristic algorithms. However, the CPU time of the exact method increases exponentially while the size of problems increases. Generally speaking, MOPSO performs better than NSGA-II in the MID and SM criteria, while NSGA-II is better than MOPSO in the DM and CPU time criteria, but the difference in the four criteria is not particularly significant.

VI. CONCLUSIONS AND FUTURE WORK

This paper discusses a robust optimization model for grid emergency goods distribution. In fact, the model presents a range of available options because of the dispersion of Pareto-optimal sets and the relationship of objectives. This research can optimally assign the amount and path of emergency goods based on sensitivity analysis of disaster situations and relationship of optimized objectives. In other words, it helps the decision makers in the power grid to distribute goods more efficiently. The following conclusions can be drawn from this article:

1) We uses the ε-constraint method to solve the multi-objective optimization problem exactly. The Pareto-optimal set shows that an increase in the total time (Obj_1) will result in an increase in the goods shortage (Obj_2) and a decrease in the total cost (Obj_3).
2) Compared with the models which cover lower degrees of uncertainty, the model considering demand, supply, and the costs of procurement and transportation as uncertain parameters increases computational complexity, so the total time increases from 1.67% to 9.65%. However, it can reduce the shortage of goods ranging from 2.04% to 8.22% and the total cost ranging from 5.94% to 15.2%.
3) We utilize ε-constraint method and two heuristic algorithms (MOPSO/ NSGA-II) to solve test problems. The CPU time of ε-constraint method is immensely affected by the size of problems. The heuristic algorithms are

performing better, which is especially more sensible when the size increases. Additionally, MOPSO and NSGA-II are comparable.

In the future, different types of vehicles and corresponding transportation costs can be considered; in addition, for large-scale problems, especially the problems that scenario types, goods types, and the number of AAs are simultaneously increased, it is necessary to propose new meta-heuristic algorithms. As a limitation, it should be noted that the proposed framework and algorithms are related to the selected case study, and we cannot be sure that these outcomes will be efficient for other areas.

REFERENCES

[1] Q. Xia, G.-X. Xu, and C.-Q. Kang, "Planning of anti-disaster power system," *Power Syst. Technol.*, vol. 33, no. 3, pp. 1–7, Feb. 2009.
[2] Y. Wang, C. Chen, J. Wang, and R. Baldick, "Research on resilience of power systems under natural disasters—A review," *IEEE Trans. Power Syst.*, vol. 31, no. 2, pp. 1604–1613, Mar. 2016.
[3] A. Arab, A. Khodaei, Z. Han, and S. K. Khator, "Proactive recovery of electric power assets for resiliency enhancement," *IEEE Access*, vol. 3, pp. 99–109, Feb. 2015.
[4] Y. Liu and C. Singh, "A methodology for evaluation of hurricane impact on composite power system reliability," *IEEE Trans. Power Syst.*, vol. 26, no. 1, pp. 145–152, Feb. 2011.
[5] M. Panteli, C. Pickering, S. Wilkinson, R. Dawson, and P. Mancarella, "Power system resilience to extreme weather: Fragility modeling, probabilistic impact assessment, and adaptation measures," *IEEE Trans. Power Syst.*, vol. 32, no. 5, pp. 3747–3757, Sep. 2017.
[6] S. Espinoza, M. Panteli, P. Mancarella, and H. Rudnick, "Multi-phase assessment and adaptation of power systems resilience to natural hazards," *Electr. Power Syst. Res.*, vol. 136, pp. 352–361, Jul. 2016.
[7] H. Luo, F. Xinyan, Y. Guoqin, and Z. Tongtong, "Analysis on auxiliary decision-making for start-up of power emergency command center under sudden events," *Power Syst. Technol.*, vol. 38, no. 4, pp. 1020–1025, Apr. 2014.
[8] C. Bian and X. Fang, "Location model of power emergency material storage considering load rating," *Proc. CSU-EPSA*, vol. 29, no. 1, pp. 78–83, Jan. 2017.
[9] H. O. Mete and Z. B. Zabinsky, "Stochastic optimization of medical supply location and distribution in disaster management," *Int. J. Prod. Econ.*, vol. 126, no. 1, pp. 76–84, Jul. 2010.
[10] X. Zhang, "Inventory control under temporal demand heteroscedasticity," *Eur. J. Oper. Res.*, vol. 182, no. 1, pp. 127–144, Oct. 2007.
[11] J.-B. Sheu, "Dynamic relief-demand management for emergency logistics operations under large-scale disasters," *Transp. Res. E, Logistics Transp. Rev.*, vol. 46, no. 1, pp. 1–17, 2010.
[12] G. L. Doorman, K. Uhlen, G. H. Kjolle, and E. S. Huse, "Vulnerability analysis of the nordic power system," *IEEE Trans. Power Syst.*, vol. 21, no. 1, pp. 402–410, Feb. 2006.
[13] J. K. Fang, C. Su, Z. Chen, H. Sun, and P. Lund, "Power system structural vulnerability assessment based on an improved maximum flow approach," *IEEE Trans. Smart Grid*, vol. 9, no. 2, pp. 777–785, Mar. 2018.
[14] G.-H. Tzeng, H.-J. Cheng, and T. D. Huang, "Multi-objective optimal planning for designing relief delivery systems," *Transp. Res. E, Logistics Transp. Rev.*, vol. 43, no. 6, pp. 673–686, Nov. 2007.
[15] A. M. Caunhye, X. Nie, and S. Pokharel, "Optimization models in emergency logistics: A literature review," *Socio-Econ. Planning Sci.*, vol. 46, no. 1, pp. 4–13, Mar. 2012.
[16] J. Zhou, F. Yang, and K. Wang, "Multi-objective optimization in uncertain random environments," *Fuzzy Optim. Decis. Making*, vol. 13, no. 4, pp. 397–413, Dec. 2014.
[17] R. M. Tomasini and L. N. Van Wassenhove, "Pan-american health organization's humanitarian supply management system: De-politicization of the humanitarian supply chain by creating accountability," *J. Public Procurement*, vol. 4, no. 3, pp. 437–449, Jan. 2004.
[18] A. Bozorgi-Amiri, M. S. Jabalameli, and S. M. J. M. Al-E-Hashem, "A multi-objective robust stochastic programming model for disaster relief logistics under uncertainty," *OR Spectr.*, vol. 35, no. 4, pp. 905–933, Nov. 2013.
[19] S. Tofighi, S. A. Torabi, and S. A. Mansouri, "Humanitarian logistics network design under mixed uncertainty," *Eur. J. Oper. Res.*, vol. 250, no. 1, pp. 239–250, Apr. 2016.
[20] P. Murali, F. Ordóñez, and M. M. Dessouky, "Facility location under demand uncertainty: Response to a large-scale bio-terror attack," *Socio-Econ. Planning Sci.*, vol. 46, no. 1, pp. 78–87, Mar. 2012.
[21] D. T. Nguyen, Y. Shen, and M. T. Thai, "Detecting critical nodes in interdependent power networks for vulnerability assessment," *IEEE Trans. Smart Grid*, vol. 4, no. 1, pp. 151–159, Mar. 2013.
[22] E. Bompard, R. Napoli, and F. Xue, "Analysis of structural vulnerabilities in power transmission grids," *Int. J. Crit. Infrastruct. Protection*, vol. 2, nos. 1–2, pp. 5–12, 2009.
[23] G. Chen, Z. Y. Dong, D. J. Hill, and G. H. Zhang, "An improved model for structural vulnerability analysis of power networks," *Phys. A, Statist. Mech. Appl.*, vol. 388, no. 9, pp. 4259–4266, Oct. 2009.
[24] M. Rezaei-Malek and R. Tavakkoli-Moghaddam, "Robust humanitarian relief logistics network planning," *Uncertain Supply Chain Manage.*, vol. 2, no. 2, pp. 73–96, Jan. 2014.
[25] W. Wu, J. Chen, B. Zhang, and H. Sun, "A robust wind power optimization method for look-ahead power dispatch," *IEEE Trans. Sustain. Energy*, vol. 5, no. 2, pp. 507–515, Apr. 2014.
[26] J. M. Mulvey, R. J. Vanderbei, and S. A. Zenios, "Robust optimization of large-scale systems," *Oper. Res.*, vol. 43, no. 2, pp. 264–281, Apr. 1995.
[27] S. Y. Balaman, "Investment planning and strategic management of sustainable systems for clean power generation: An ε-constraint based multi objective modelling approach," *J. Cleaner Prod.*, vol. 137, pp. 1179–1190, Nov. 2016.
[28] M. Haghi, S. M. T. F. Ghomi, and F. Jolai, "Developing a robust multi-objective model for pre/post disaster times under uncertainty in demand and resource," *J. Cleaner Prod.*, vol. 154, pp. 188–202, Jun. 2017.
[29] K. Deb, A. Pratap, S. Agarwal, and T. Meyarivan, "A fast and elitist multiobjective genetic algorithm: NSGA-II," *IEEE Trans. Evol. Comput.*, vol. 6, no. 2, pp. 182–197, Apr. 2002.
[30] S. M. K. Heris and H. Khaloozadeh, "Open- and closed-loop multiobjective optimal strategies for HIV therapy using NSGA-II," *IEEE Trans. Biomed. Eng.*, vol. 58, no. 6, pp. 1678–1685, Jun. 2011.
[31] H. M. Alsaket, K. R. Mahmoud, H. M. Elattar, and M. A. Aboul-Dahab, "Exploring evolutionary multi-objective techniques in self-organizing networks," *IEEE Access*, vol. 5, pp. 12049–12060, May 2017.
[32] L. Zuo, L. Shu, S. Dong, C. Zhu, and T. Hara, "A multi-objective optimization scheduling method based on the ant colony algorithm in cloud computing," *IEEE Access*, vol. 3, pp. 2687–2699, Dec. 2015.
[33] B. Vahdani, D. Veysmoradi, F. Noori, and F. Mansour, "Two-stage multi-objective location-routing-inventory model for humanitarian logistics network design under uncertainty," *Int. J. Disaster Risk Reduction*, vol. 27, pp. 290–306, Mar. 2018.
[34] E. Zitzler, K. Deb, and L. Thiele, "Comparison of multiobjective evolutionary algorithms: Empirical results," *Evol. Comput.*, vol. 8, no. 2, pp. 173–195, 2000.
[35] M. Rabbani, M. A. Bajestani, and G. B. Khoshkhou, "A multi-objective particle swarm optimization for project selection problem," *Expert Syst. Appl.*, vol. 37, no. 1, pp. 315–321, Jan. 2010.

YIWEN JIANG was born in Yiwu, Zhejiang, China, in 1995. She received the bachelor's degree from the Department of Electronics and Information Engineering, Huazhong University of Science and Technology, Wuhan, China, in 2017, where she is currently pursuing the master's degree. Her interests include the engineering optimization, condition monitoring, and deep learning in the power grid.

LEE LI (SM'17) was born in Jingzhou, Hubei, China, in 1976. He received the Ph.D. degree from the Department of Electronics and Information Engineering, Huazhong University of Science and Technology (HUST), Wuhan, China, in 2006. He is currently an Associate Professor with the College of Electrical and Electronic Engineering, HUST. His interests include data mining technologies of power engineering, integrative management of power grid, condition monitoring and assessment of power equipments.

ZHENSHENG LIU was born in Chengzhou, Hunan, China, in 1976. He received the bachelor's degree from the Department of Electronics and Information Engineering, Huazhong University of Science and Technology, Wuhan, China, in 2017, where he is currently pursuing the master's degree. His interests include high voltage and insulation technology.